

K-BAND SPECTROSCOPY OF AN OBSCURED MASSIVE STELLAR CLUSTER IN THE ANTENNAE GALAXIES (NGC 4038/4039) WITH NIRSPEC¹

ANDREA M. GILBERT^{2,8}, JAMES R. GRAHAM², IAN S. MCLEAN³, E. E. BECKLIN³, DONALD F. FIGER⁴, JAMES E. LARKIN³, N. A. LEVENSON⁵, HARRY I. TEPLITZ^{6,7}, MAVOURNEEN K. WILCOX³

To appear in ApJL; submitted Oct. 27, 1999

ABSTRACT

We present infrared spectroscopy of the Antennae Galaxies (NGC 4038/4039) with NIRSPEC at the W. M. Keck Observatory. We imaged the star clusters in the vicinity of the southern nucleus (NGC 4039) in 0".39 seeing in K-band using NIRSPEC's slit-viewing camera. The brightest star cluster revealed in the near-IR ($M_K(0) \simeq -17.9$) is insignificant optically, but coincident with the highest surface brightness peak in the mid-IR (12–18 μ m) ISO image presented by Mirabel et al. (1998). We obtained high signal-to-noise 2.03–2.45 μ m spectra of the nucleus and the obscured star cluster at $R \sim 1900$.

The cluster is very young (age ~ 4 Myr), massive ($M \sim 16 \times 10^6 M_\odot$), and compact (density $\sim 115 M_\odot \text{ pc}^{-3}$ within a 32 pc half-light radius), assuming a Salpeter IMF (0.1–100 M_\odot). Its hot stars have a radiation field characterized by $T_{\text{eff}} \sim 39,000$ K, and they ionize a compact H II region with $n_e \sim 10^4 \text{ cm}^{-3}$. The stars are deeply embedded in gas and dust ($A_V \sim 9 - 10$ mag), and their strong FUV field powers a clumpy photodissociation region with densities $n_H \gtrsim 10^5 \text{ cm}^{-3}$ on scales of ~ 200 pc, radiating $L_{\text{H}21-0 \text{ S}(1)} = 9600 L_\odot$.

Subject headings: galaxies: individual (NGC4038/39, Antennae Galaxies) — galaxies: ISM — galaxies: starburst — galaxies: star clusters — infrared: galaxies — H II regions

1. INTRODUCTION

The Antennae (NGC 4038/4039) are a pair of disk galaxies in an early stage of merging which contain numerous massive super star clusters (SSCs) along their spiral arms and around their interaction region (Whitmore & Schweizer, 1995; Whitmore et al., 1999). The molecular gas distribution peaks at both nuclei and in the overlap region (Stanford et al., 1990), but the gas is not yet undergoing a global starburst typical of more advanced mergers (Nikola et al., 1998). Star formation in starbursts appears to occur preferentially in SSCs. We chose to observe the Antennae because their proximity permits an unusually detailed view of the first generation of merger-induced SSCs and their influence on the surrounding interstellar medium.

The Infrared Space Observatory (ISO) 12–18 μ m image showed that the hot dust distribution is similar to that of the gas, but peaks at an otherwise inconspicuous point on the southern edge of the overlap region (Mirabel et al., 1998). This powerful starburst knot is also a flat-spectrum radio continuum source (Hummel & van der Hulst, 1986) and may be associated with an X-ray source (Fabbiano et al., 1997). We imaged the region around this knot, and discovered a bright compact star cluster coincident with the mid-IR peak. We obtained moderate-resolution (R

~ 1900) K-band spectra of both the obscured cluster and the NGC 4039 nucleus.

2. OBSERVATIONS & DATA REDUCTION

NIRSPEC is a new facility infrared (0.95–5.6 μ m) spectrometer for the Keck-II telescope, commissioned during April through July, 1999 (McLean et al., 1998). It has a cross-dispersed cryogenic echelle with $R \sim 25,000$, and a low resolution mode with $R \sim 2000$. The spectrometer detector is a 1024×1024 InSb ALADDIN focal plane array, and the IR slit-viewing camera detector is a 256×256 HgCdTe PICNIC array.

We observed the Antennae with NIRSPEC during the June 1999 commissioning run. Slit-viewing camera (SCAM) images at 2 μ m reveal that the mid-IR ISO peak is a bright ($K = 14.6$) compact star cluster located 20".4 east and 4".7 north of the K-band nucleus. This cluster is associated with a faint ($V = 23.5$) red ($V-I = 2.9$) source (# 80 in Whitmore & Schweizer 1995) visible with Space Telescope (Whitmore & Zhang, private communication). We obtained low resolution ($R \simeq 1900$) $\lambda \simeq 2.03 - 2.45 \mu$ m spectra through a $0''.57 \times 42''$ slit at $\text{PA} = 77^\circ$ located on the obscured star cluster and the nucleus of NGC 4039. The total integration time on source was 2100 s.

We dark-subtracted, mean-sky-subtracted, flat-fielded,

¹Data presented herein were obtained at the W.M. Keck Observatory, which is operated as a scientific partnership among the California Institute of Technology, the University of California and the National Aeronautics and Space Administration. The Observatory was made possible by the generous financial support of the W.M. Keck Foundation.

² Department of Astronomy, University of California, 601 Campbell Hall, Berkeley, CA, 94720-3411

³ Department of Physics and Astronomy, University of California, Los Angeles, CA, 90095-1562

⁴ Space Telescope Science Institute, 3700 San Martin Dr., Baltimore, MD 21218

⁵ Department of Physics and Astronomy, Johns Hopkins University, Baltimore, MD 21218

⁶ Laboratory for Astronomy and Solar Physics, Code 681, Goddard Space Flight Center, Greenbelt MD 20771

⁷ NAO Research Associate

⁸ agilbert@astro.berkeley.edu

and corrected two-dimensional spectra for bad pixels and cosmic rays before rectifying the curved order onto a grid in which wavelength and slit position are perpendicular. We then corrected for residual sky emission and divided by a B1.5 standard star spectrum to correct for atmospheric absorption. The object spectra were extracted using a Gaussian weighting function matched to their strong continua collapsed in wavelength (intrinsic FWHM = $0''.84$ for cluster, $0''.99$ for nucleus)⁹, and then an aperture correction was applied to recover the full flux in the continua. Thus we neglected more-extended H₂ emission, which has maximum FWHM $\sim 1''.7$ in the cluster and $\sim 1''.2$ in the nucleus. We obtained a flux scale by requiring the $2.2\ \mu\text{m}$ star flux to equal that corresponding to its K magnitude. Reduced spectra are shown in Figures 1 and 2.

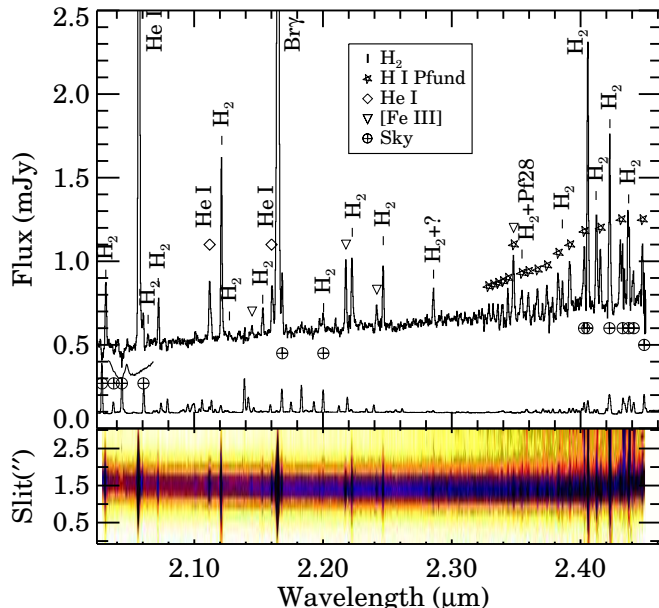


Figure 1. - NIRSPEC spectrum of the obscured star cluster shows nebular and fluorescent H₂ emission with a continuum rising toward the red. Scaled sky counts are plotted at 0.1 mJy. ω -shaped curve represents an atmospheric CO₂ band at $2.05\ \mu\text{m}$.

3. MASSIVE STAR CLUSTER

The cluster spectrum is characterized by strong emission lines¹⁰ and a continuum (detected with SNR $\simeq 15$) dominated by the light of hot, blue stars and dust. The nebular emission lines are slightly more extended than the continuum, and the H₂ emission is even more extended. This suggests a picture in which hot stars and dust are embedded in a giant compact H II region surrounded by clumpy (see §3.2) clouds of obscuring gas and dust whose surfaces are ionized and photodissociated by FUV photons escaping from the star cluster.

For a distance to the Antennae of 19 Mpc ($H_0=75\ \text{km s}^{-1}\ \text{Mpc}^{-1}$, $1''=93\ \text{pc}$) (Whitmore et al., 1999), we find that the cluster has $M_K = -16.8$. We estimate the screen extinction to the cluster by assuming a range of $(V-K)_0 \simeq 0 - 1$ as expected from Starburst99 models (Leitherer et al., 1999), and that $A_K = 0.11\ A_V$ (Rieke & Lebofsky, 1985). We find $A_V = 9 - 10\ \text{mag}$, which implies $M_K(0) = -17.9$, adopting $A_K = 1.1$ (which is con-

firmed by our analysis of the H II recombination lines in §3.1). We can use the intrinsic brightness along with the Lyman continuum flux inferred from the de-reddened Br γ flux ($3.1 \times 10^{-14}\ \text{erg s}^{-1}\ \text{cm}^{-2}$), $Q(\text{H}^+)_0 = 1.0 \times 10^{53}\ \text{photons s}^{-1}$, to constrain the cluster mass and age. Using instantaneous Starburst99 models we find a total mass of $\sim 7 \times 10^6\ M_\odot$ (with $\sim 2600\ \text{O stars}$) for a Salpeter IMF extending from 1 to $100\ M_\odot$, and an age of $\sim 4\ \text{Myr}$. This age is consistent with the lack of photospheric CO and metal absorption lines from red supergiants and other cool giants, which would begin to contribute significantly to the $2\ \mu\text{m}$ light at an age of $\sim 7\ \text{Myr}$ (Leitherer et al., 1999). The cluster's density is then about $115\ M_\odot\ \text{pc}^{-3}$ for stars of $0.1 - 100\ M_\odot$ within a half-light radius of 32 pc. This density is 30 times less than that of the LMC SSC, R136 (within a radius of 1.7 pc, assuming a Salpeter proportion of low-mass stars) (Hunter et al., 1995). Thus the Antennae cluster may be a complex of clusters rather than one massive cluster.

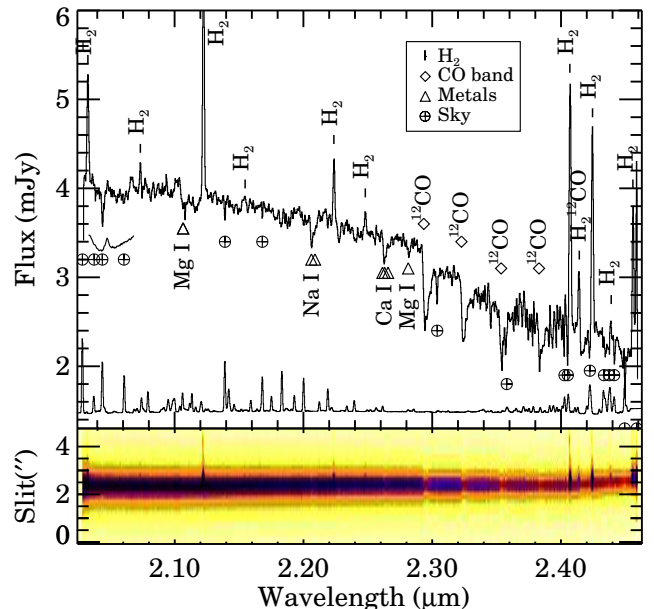


Figure 2. - NIRSPEC spectrum of NGC 4039 nucleus shows extended collisionally excited H₂ emission and a strong stellar continuum marked by photospheric absorption. No Br γ is present. Scaled sky counts are shown at 1.5 mJy.

3.1. Nebular Emission

The cluster spectrum features a variety of nebular lines that reveal information about the conditions in the ionized gas around the cluster, which in turn allows us to constrain the effective temperature of the ionizing stars.

We detected H I Pfund series lines from Pf 19 to Pf 38, and display their fluxes relative to that of Br γ in Figure 3. The filled symbols give fluxes for the blends Pf 28+H₂ 2-1 S(0) and Pf 29+[Fe III]. They fall well above the other points, which follow closely the theoretical expectation for intensities relative to Br γ (solid curve) with no reddening applied, for a gas with $n_e = 10^4\ \text{cm}^{-3}$ and $T_e = 10^4\ \text{K}$ (Hummer & Storey, 1987). Excluding the two known blends, the best-fit foreground screen extinction is $A_K = 1.1 \pm 0.3\ \text{mag}$ (dashed curve), assuming the

⁹These widths are greater than those measured from the SCAM images, $\sim 0''.69$ and $\sim 0''.83$ (intrinsic), due to the extended line contribution and rectification errors of order $\lesssim 1$ pixel at the chip edges.

¹⁰A table of measured line fluxes is available electronically from <http://astro.berkeley.edu/~agilbert/antennae>.

extinction law of Landini et al. (1984) and evaluated at $2.2 \mu\text{m}$. We consider this an upper limit on A_K because a close look at the spectrum shows that the points above the dashed line in Figure 3 for Pf 22–24 at 2.404 , 2.393 , and $2.383 \mu\text{m}$ may also be blended or contaminated by sky emission, implying a lower A_K and a much better fit to the theory. Hence the majority of the extinction to the cluster is bypassed by observing it in K band.

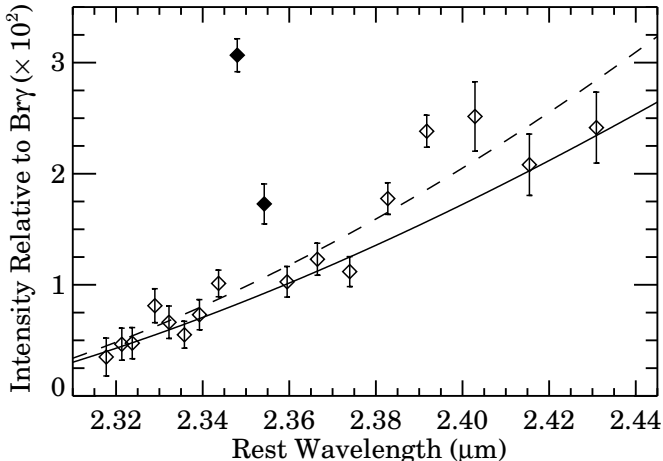


Figure 3. - Pfund line fluxes relative to Br γ flux ($1.05 \times 10^{-14} \text{ erg s}^{-1} \text{ cm}^{-2}$). Solid curve is unextinguished theoretical curve for $n_e = 10^4 \text{ cm}^{-3}$, $T_e = 10^4 \text{ K}$ (Hummer & Storey 1987). Filled symbols represent lines that are known blends, and the dashed curve shows theoretical fluxes with the best-fit extinction $A_K = 1.1 \text{ mag}$.

The lack of a strong Pfund discontinuity at $2.28 \mu\text{m}$ indicates that nebular free-free and bound-free continuum is diluted by starlight and dust emission (signaled by the rising continuum toward longer λ) in the cluster.

The ratios of [Fe III] lines are nebular density diagnostics; Table 1 presents observed ratios and theoretical predictions of Keenan et al. (1992) for emission from a collisionally excited 10^4 K gas, as tabulated by Luhman et al. (1998). The ratios of [Fe III] $2.146 \mu\text{m}$ and [Fe III] $2.243 \mu\text{m}$ to [Fe III] $2.218 \mu\text{m}$ are consistent with $n_e = 10^{3.5} - 10^4 \text{ cm}^{-3}$. The ratio [Fe III] $2.348 \mu\text{m}$ /[Fe III] $2.218 \mu\text{m}$ is 20% higher than its theoretical value, which is roughly constant over all of parameter space (Keenan et al., 1992), but [Fe III] $2.348 \mu\text{m}$ is blended with Pf 29 and subject to measurement errors that are larger than the difference in extinctions in question (see Figure 3). Even the minimum value we infer for this ratio, with $A_K = 0$, is significantly greater than the model prediction. High values of [Fe III] $2.348 \mu\text{m}$ /[Fe III] $2.218 \mu\text{m}$ were also found by Luhman et al. (1998) in Orion. This discrepancy may be due to blending with another unknown line, or to theoretical error; ratios from the latest calculations have an average deviation from data of 10% (Keenan et al., 1992).

He I line ratios can in principal be used to infer nebular temperature T_e , and are fairly insensitive to n_e . However, of the three lines we detected, two are not suitable for such an analysis: the He I $2.1615 + 2.1624 \mu\text{m}$ blend falls on the wing of strong Br γ so its flux has a large (50%) measurement error, and the strong He I $2.0589 \mu\text{m}$ line is subject to radiative transfer and density effects.

The He I $2.0589 \mu\text{m}$ /Br γ ratio is an indicator of the T_{eff} of hot stars in H II regions (Doyon et al., 1992), although it is sensitive to nebular conditions such as the relative

volumes and ionization fractions of He $^+$ and H $^+$, geometry, density, dustiness, etc. (Shields, 1993). Doherty et al. (1995) studied H and He excitation in a sample of starburst galaxies and H II regions. For starbursts they found evidence for high- T_{eff} , low- n_e ($\sim 10^2 \text{ cm}^{-2}$) ionized gas from He I $2.0589 \mu\text{m}$ /Br γ ratios of 0.22 to 0.64. This is consistent with giant extended H II regions expected to dominate the emission-line spectra of typical starbursts. The ultra-compact H II regions were characterized by higher ratios (0.8–0.9) and higher densities, $\sim 10^4 \text{ cm}^{-3}$. The cluster has a flux ratio of 0.70, a value between the two object classes of Doherty et al. (1995). Assuming the line emission is purely nebular, this ratio is consistent with a high-density (10^4 cm^{-3}) model of Shields (1993), and implies $T_{\text{eff}} \simeq 39,000 \text{ K}$ for the assumed model parameters. This temperature is similar to that derived by Kunze et al. (1996), $\simeq 44,000 \text{ K}$, from mid-IR SWS line observations in a large aperture on the overlap region of the Antennae.

TABLE 1
CLUSTER [Fe III] LINE RATIOS^a

| Transition | Rest $\lambda(\mu\text{m})^b$ | Observed Ratio | Model Ratio ^c | | |
|-------------------------------|-------------------------------|-------------------|--------------------------|--------|--------|
| | | | 10^3 | 10^4 | 10^5 |
| $^3\text{G}_3 - ^3\text{H}_4$ | 2.1457 | 0.14 ± 0.02 | 0.10 | 0.17 | 0.34 |
| $^3\text{G}_5 - ^3\text{H}_6$ | 2.2183 | 1.00 | 1.00 | 1.00 | 1.00 |
| $^3\text{G}_4 - ^3\text{H}_4$ | 2.2427 | 0.28 ± 0.02 | 0.26 | 0.29 | 0.38 |
| $^3\text{G}_5 - ^3\text{H}_5$ | 2.3485 | 0.80 ± 0.03^d | 0.66 | 0.66 | 0.66 |

^a Ratios are dereddened fluxes relative to [Fe III] $2.2183 \mu\text{m}$, for which the dereddened flux was $9.11 \times 10^{-16} \text{ ergs s}^{-1} \text{ cm}^{-2}$.

^b Sugar & Corliss (1985).

^c Models for $T_e = 10^4 \text{ K}$, values of n_e in cm^{-3} (Keenan et al., 1992).

^d Flux determined by subtracting Pf 29 contribution obtained for the best-fit Landini extinction curve with $A_K = 1.1 \text{ mag}$.

The cluster has properties more like those of a compact H II region than a diffuse one. It appears to be a young, hot, high-density H II region, one of the first to form in this part of the Antennae interaction region (see Habing & Israel 1979 for a review of compact H II regions).

3.2. Molecular Emission

The spectrum shows evidence for almost pure UV fluorescence excited by FUV radiation from the O & B stars; the strong, vibrationally excited 1–0, 2–1 & 3–2 H $_2$ emission has $T_{\text{vib}} \gtrsim 6000 \text{ K}$ and $T_{\text{rot}} \simeq 970, 1600$, and 1800 K , respectively, and weak higher- v (6–4, 8–6, 9–7) transitions are present as well. The H $_2$ lines are extended over $\simeq 200 \text{ pc}$, about twice the extent of the continuum and nebular line emission, so a significant fraction of the FUV (912–1108 Å) light escapes from the cluster to heat and photodissociate the local molecular ISM.

We obtained the photodissociation region (PDR) models of Draine & Bertoldi (1996) and compared them with our data by calculating reduced χ^2_ν . Models with high densities ($n_H = 10^5 \text{ cm}^{-3}$), moderately warm temperatures ($T = 500$ to 1500 K at the cloud surface), and high FUV fields ($G_0 = 10^3 - 10^5$ times the mean interstellar field) can reasonably fit the data. Figure 4 shows χ^2_ν contours for all models projected onto the $n_H - G_0$ plane. The best-fit Draine & Bertoldi model is n2023b, which has $n_H = 10^5 \text{ cm}^{-3}$, $T = 900 \text{ K}$, and $G_0 = 5000$. We fit 22 H $_2$ lines, excluding 3–2 S(2) $2.287 \mu\text{m}$ because it appears to be blended with a strong unidentified nebular line at 2.286

μm found in higher-resolution spectra of planetary nebulae (Smith et al., 1981). The weak high- v transitions are all under-predicted by this model, and appear to come from lower-density gas ($n_{\text{H}} \lesssim 10^3 - 10^4 \text{ cm}^{-3}$) exposed to a weaker FUV field ($G_0 \lesssim 10^2 - 10^3$).

The ortho/para ratio of excited H_2 determined from the relative column densities in $v=1, J=3$ and $J=2$ inferred from 1–0 S(1) and S(0) lines is 1.62 ± 0.07 . This is consistent with the ground state $v=0, J=1$ and $J=0$ H_2 being in LTE with ortho/para ratio of 3 if the FUV absorption lines populating the non-LTE excited states are optically thick (Sternberg & Neufeld, 1999). Indeed, the best-fit PDR models have temperatures that are comparable with T_{rot} in the lowest excited states, as well as with the warm gas kinetic temperature in the Galactic PDR M16, $T = 930 \pm 50 \text{ K}$, measured by Levenson et al. (1999).

If the extent of the H_2 emission indicates that the mean-free path of a FUV photon is $\sim 200 \text{ pc}$, then $\langle n_{\text{H}} \rangle = 3 \text{ cm}^{-3}$ for a Galactic gas-to-dust ratio, while in the PDR(s) $n_{\text{H}} = 10^4 - 10^6 \text{ cm}^{-3}$. This implies that the molecular gas is extremely clumpy, which is consistent with the range of densities inferred from the detection of anomalously strong $v = 8-6$ H_2 emission.

4. NGC 4039 NUCLEUS

The spectrum of the nucleus of NGC 4039 is marked by strong stellar continuum and bright, extended H_2 emission. Strong photospheric Mg I, Na I, Ca I absorption and CO $\Delta v = 2$ bands indicate that the continuum is dominated by old giants. The CO band head is stronger than that of a M2III, suggesting some contribution from red supergiants. The absence of Br γ emission implies that star formation is currently extinct in the nucleus. Spatially extended, collisionally excited H_2 emission in the nucleus may be excited by SNR shocks from the last generation of nuclear star formation, or by merger-induced cloud collisions. We defer detailed analysis of the nuclear spectrum to a later paper.

5. CONCLUSIONS

The highest surface brightness mid-IR peak in the ISO map of the Antennae Galaxies is a massive ($\sim 16 \times 10^6 M_{\odot}$), obscured ($A_V \sim 9 - 10$), young (age $\sim 4 \text{ Myr}$) star cluster with half-light radius $\sim 32 \text{ pc}$, whose strong FUV flux excites the surrounding molecular ISM on scales of up to 200 pc. The cluster spectrum is dominated by

extended fluorescently excited H_2 emission from clumpy PDRs and nebular emission from compact H II regions. In contrast, the nearby nucleus of NGC 4039 has a strong stellar spectrum dominated by cool stars, where the only emission lines are due to shock-excited H_2 . These observations confirm the potential of near-infrared spectroscopy for exploration and discovery with the new generation of large ground-based telescopes. Our ongoing program of NIRSPEC observations promises to reveal a wealth of information on the nature of star formation in star clusters.

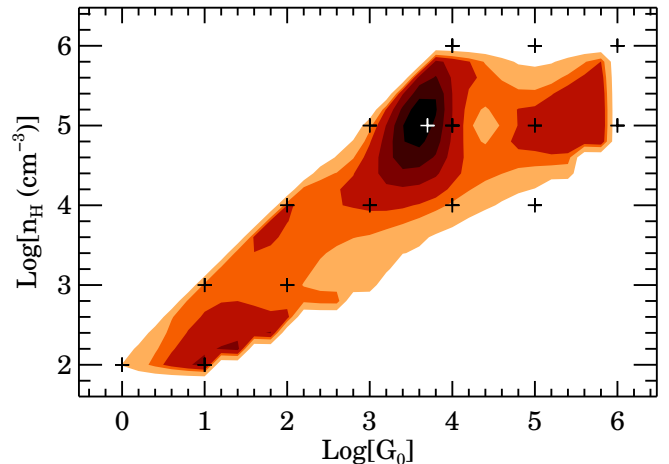


Figure 4. - Comparison of H_2 line strengths with PDR models. Contours of χ^2_{ν} for 22 lines projected onto $n_{\text{H}}-G_0$ plane peak at $n_{\text{H}} \sim 10^5 \text{ cm}^{-3}$ and $G_0 \sim 5000$. Model points (+) are for $T_0 = 300 - 2000 \text{ K}$. White + marks best-fit PDR model of Draine & Bertoldi, with $T_0 = 900 \text{ K}$ and $\chi^2_{\nu} = 9.3$. Contours are 50, 25, 20, 15, 12, 10.

We acknowledge the hard work of past and present members of the UCLA NIRSPEC team: M. Anglione, O. Bendiksen, G. Brims, L. Buchholz, J. Canfield, K. Chin, J. Hare, F. Lacayanga, S. Larson, T. Liu, N. Magnone, G. Skulason, M. Spencer, J. Weiss and W. Wong. We thank Keck Director Chaffee and all the CARA staff involved in the commissioning and integration of NIRSPEC, particularly instrument specialist T. Bida. We especially thank Observing Assistants J. Aycock, G. Puniwai, C. Sorenson, R. Quick and W. Wack for their support. We also thank A. Sternberg for valuable discussions. We are grateful to R. Benjamin for providing us with He I emissivity data. AMG acknowledges support from a NASA GSRP grant.

REFERENCES

- Doherty, R. M., Puxley, P. J., Lumsden, S. L., & Doyon, R. 1995, MNRAS, 277, 577
Doyon, R., Puxley, P. J., & Joseph, R. D. 1992, ApJ, 397, 117
Draine, B. T. & Bertoldi, F. 1996, ApJ, 468, 269
Fabbiano, G., Schweizer, F., & Mackie, G. 1997, ApJ, 478, 542
Habing, H. J. & Israel, F. P. 1979, ARA&A, 17, 345
Hummel, E. & van der Hulst, J. M. 1986, A&A, 155, 151
Hummer, D. G. & Storey, P. J. 1987, MNRAS, 224, 801
Hunter, D. A., Shaya, E. J., Holtzman, J. A., Light, R. M., O’Neil, E. J., & Lynds, R. 1995, ApJ, 448, 179
Keenan, F. P., Berrington, K. A., Burke, P. G., Zeippen, C. J., Le Dourneuf, M., & Clegg, R. E. S. 1992, ApJ, 384, 385
Kunze, D., et al. 1996, A&A, 315, L101
Landini, M., Natta, A., Salinari, P., Oliva, E., & Moorwood, A. F. M. 1984, A&A, 134, 284
Leitherer, C., et al. 1999, ApJS, 123, 3
Levenson, N. A., et al. 2000, to appear in ApJL
Luhman, K. L., Engelbracht, C. W., & Luhman, M. L. 1998, ApJ, 499, 799
McLean, I. S., et al. 1998, Proc. SPIE, 3354, 566
Mirabel, I. F., et al. 1998, A&A, 333, L1
Nikola, T., Genzel, R., Herrmann, F., Madden, S. C., Poglitsch, A., Geis, N., Townes, C. H., & Stacey, G. J. 1998, ApJ, 504, 749
Rieke, G. H. & Lebofsky, M. J. 1985, ApJ, 288, 618
Shields, J. C. 1993, ApJ, 419, 181
Smith, H. A., Larson, H. P., & Fink, U. 1981, ApJ, 244, 835
Stanford, S. A., Sargent, A. I., Sanders, D. B., & Scoville, N. Z. 1990, ApJ, 349, 492
Sternberg, A. & Neufeld, D. A. 1999, ApJ, 516, 371
Sugar, J. & Corliss, C. 1985, Atomic energy levels of the iron-period elements: Potassium through Nickel (Washington: American Chemical Society, 1985)
Whitmore, B. C. & Schweizer, F. 1995, AJ, 109, 960
Whitmore, B. C., Zhang, Q., Leitherer, C., Fall, S. M., Schweizer, F., & Miller, B. W. 1999, AJ